PNAS RESEARCH ARTICLE | MICROBIOLOGY

Bioremediation of mercury-polluted soil and water by the plant symbiotic fungus *Metarhizium robertsii*

Congcong Wu[a], Dan Tang[a], Jin Dai[a], Xingyuan Tang[a], Yuting Bao[a], Jiali Ning[a], Qing Zhen[a], Hui Song[a], Raymond J. St. Leger[b], and Weiguo Fang[a,1]

Edited by Mary Lou Guerinot, Dartmouth College, Hanover, NH; received August 24, 2022; accepted October 17, 2022

Fungi are central to every terrestrial and many aquatic ecosystems, but the mechanisms underlying fungal tolerance to mercury, a global pollutant, remain unknown. Here, we show that the plant symbiotic fungus *Metarhizium robertsii* degrades methylmercury and reduces divalent mercury, decreasing mercury accumulation in plants and greatly increasing their growth in contaminated soils. *M. robertsii* does this by demethylating methylmercury via a methylmercury demethylase (MMD) and using a mercury ion reductase (MIR) to reduce divalent mercury to volatile elemental mercury. *M. robertsii* can also remove methylmercury and divalent mercury from fresh and sea water even in the absence of added nutrients. Overexpression of MMD and MIR significantly improved the ability of *M. robertsii* to bioremediate soil and water contaminated with methylmercury and divalent mercury. MIR homologs, and thereby divalent mercury tolerance, are widespread in fungi. In contrast, MMD homologs were patchily distributed among the few plant associates and soil fungi that were also able to demethylate methylmercury. Phylogenetic analysis suggests that fungi could have acquired methylmercury demethylase genes from bacteria via two independent horizontal gene transfer events. Heterologous expression of MMD in fungi that lack MMD homologs enabled them to demethylate methylmercury. Our work reveals the mechanisms underlying mercury tolerance in fungi, and may provide a cheap and environmentally friendly means of cleaning up mercury pollution.

fungi | *Metarhizium* | mercury tolerance | bioremediation

Significance

Mercury pollution of soil and water worldwide is a major threat to public health, food chains, and agriculture. Bioremediation is an environmentally friendly solution. Here, we report molecular mechanisms underlying mercury tolerance in the plant symbiotic fungus *Metarhizium robertsii*. In mercury-polluted soil, this fungus, nourished by plant-derived nutrients, demethylates methylmercury via a demethylase and volatilizes divalent mercury using a reductase. Persistently removing mercury from soil in this manner decreases its accumulation in plants and increases plant growth. *Metarhizium* can also remove mercury from nutrient-free fresh and sea water. Genetic engineering was used to further improve the ability of *M. robertsii* to bioremediate mercury-polluted soil and water, facilitating its potential use in helping manage a complex set of dangerous environmental trends.

Mercury is a heavy-metal constituent of the Earth's crust that is released naturally through weathering, geothermal activities, and forest fires. However, release, and subsequent mercury pollution of soils, groundwater, rivers, and marine ecosystems worldwide, has been greatly accelerated by recent anthropogenic activities, such as mining and fossil fuel combustion (1). Furthermore, as global temperatures rise, the thawing permafrost is releasing mercury into the environment that had been trapped in the frozen ground at levels nearly twice as high as all other soils plus the ocean and atmosphere combined (2).

Mercury is toxic to almost all living organisms through its interactions with sulfhydryl, phosphoryl, carboxyl, amide, and amine groups. It is considered to be one of the three most dangerous metal elements by the US Government Agency for Toxic Substances and Disease Registry (3), and the World Health Organization includes mercury in its list of the 10 chemicals of major public health (4). Mercury is the only element to have its own environmental convention, the Minamata Convention on Mercury, which aims for a global effort for managing the risk presented by mercury to human health and the environment (5).

Organic mercury complexes are more toxic than the inorganic salts as, being lipid-soluble, they are more easily absorbed by animals and plants. In particular, the neurotoxin methylmercury (MeHg) is the only form of mercury that is augmented in food chains (6), and it comprises the majority of total mercury in top predators (7). Some bacteria resist mercury poisoning using a demethylase to convert MeHg into divalent mercury (Hg^{2+}), which is further reduced to the volatile elemental mercury (Hg^0) (8). Tolerance to diverse toxic chemicals may also be a prerequisite for the diverse ecological roles of fungal species. A feature of cosmopolitan and plant symbiotic *Metarhizium* species is that they are often found in strongly metal-polluted areas (9), and they share their tolerance to metals with mycorrhizal fungi (10). This suggests that root-colonizing fungi, so essential for much of plant life, have evolved a tolerance to metals which could add additional benefit to their symbiotic associations with plants. In this study, we identified an MeHg demethylase and an Hg^{2+} reductase which provided a plant symbiotic strain of *Metarhizium robertsii* and its plant hosts with mercury resistance. We further improved the ability of *M. robertsii* to bioremediate MeHg- and Hg^{2+}-polluted soil and water via genetic engineering, and developed feasible approaches to use this fungus to clean up MeHg and Hg^{2+} in soil and water.

Author affiliations: [a]Ministry of Education Key Laboratory of Biosystem Homeostasis and Protection, Institute of Microbiology, College of Life Science, Zhejiang University, Hangzhou 310058, China; and [b]Department of Entomology, University of Maryland, College Park, MD 20742

Author contributions: C.W. and W.F. designed research; C.W., D.T., J.D., X.T., Y.B., J.N., Q.Z., and H.S. performed research; C.W., D.T., and J.D. analyzed data; and C.W., R.J.S.L., and W.F. wrote the paper.

The authors declare no conflict of interest.

This article is a PNAS Direct Submission.

[1]To whom correspondence may be addressed. Email: wfang1@zju.edu.cn.

This article contains supporting information online at http://www.pnas.org/lookup/suppl/doi:10.1073/pnas.2214513119/-/DCSupplemental.

Published November 14, 2022.

Results

Identification of the MeHg Demethylase MMD and the Hg^{2+} Reductase MIR. Our previous genome-wide search for horizontal gene transfer events in *Metarhizium* identified a putative alkylmercury lyase (MAA_09685) potentially acquired from bacteria (11). In particular, MAA_09685 showed significant similarity to the functionally characterized bacterial MeHg demethylase MerB (12). To investigate whether MAA_09685 retains its ancestral function, we expressed it in *Escherichia coli* (*SI Appendix*, Fig. S1). We confirmed that the expressed protein increased bacterial resistance to MeHg (Fig. 1), and that the purified recombinant protein removed the methyl group from MeHg to produce Hg^{2+} with a K_m value of 3.88 ± 0.387 μM and a maximum uptake rate (V_{max}) of 2.81 ± 0.131 μmol·mg^{-1}·min^{-1} (Fig. 1 and *SI Appendix*, Fig. S1). We therefore designated MAA_09685 as an MMD (methylmercury demethylase).

MerB works with the Hg^{2+} reductase *MerA* to achieve mercury resistance in bacteria (8). Homologs of MerA were found in many fungi, including mycorrhizal fungi such as *Rhizophagus irregularis* (*SI Appendix*, Fig. S2). Expression of the *M. robertsii* homolog MAA_07932 (designated MIR; mercury ion reductase), increased the resistance of *E. coli* to Hg^{2+} (Fig. 1), and the recombinant protein reduced Hg^{2+} to Hg^0 with a K_m value of 5.42 ± 0.568 μM and a V_{max} of 6.92 ± 0.304 μmol·mg^{-1}·min^{-1} (Fig. 1 and *SI Appendix*, Fig. S1).

Supplementing growth medium with MeHg (50 μg/L) caused *M. robertsii* to increase expression of *Mmd* 6.1-fold, while *Mir* expression was up-regulated 6.9-fold by Hg^{2+} (10 mg/L). However, MeHg had no impact on *Mir* expression, and Hg^{2+} did not impact *Mmd* expression (*SI Appendix*, Fig. S3).

MMD and MIR Are Involved in Tolerance to Mercury. We constructed the single–gene deletion mutants Δ*Mmd* and Δ*Mir* and the double–gene deletion mutant Δ*Mmd*::Δ*Mir* to investigate the roles of *Mmd* and *Mir* in *M. robertsii*'s tolerance to mercury. We also constructed Mmd^{OE} overexpressing *Mmd*, Mir^{OE} overexpressing *Mir*, and Mmd^{OE}::Mir^{OE} overexpressing both *Mmd* and *Mir* (*SI Appendix*, Fig. S4). For details of these strains, see *SI Appendix*, Table S1.

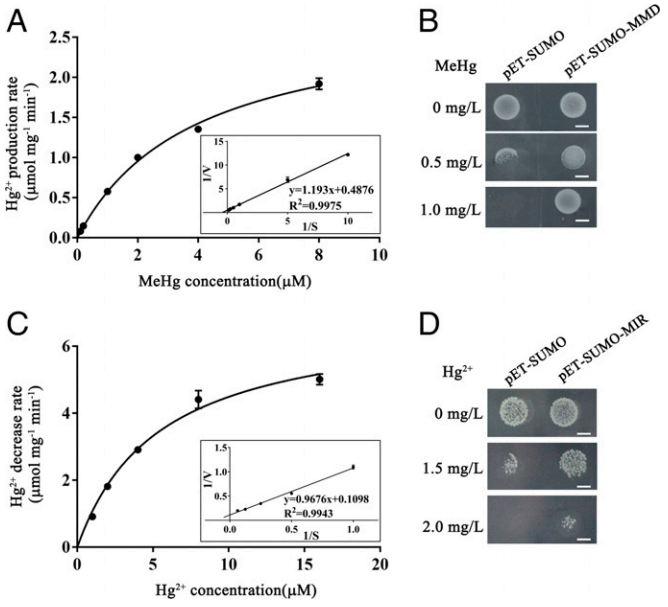

Fig. 1. Biochemical characterization of MMD and MIR. (*A*) Enzyme kinetics of MMD. (*A*, *Inset*) A Lineweaver–Burk plot of a K_m determination. (*B*) Expression of MMD increased *E. coli* tolerance to MeHg. The proteins expressed are indicated (*Top*). (*C*) Enzyme kinetics of MIR. (*D*) Expression of MIR improved the tolerance of *E. coli* to Hg^{2+}. Pictures were taken 2 dpi. (Scale bar, 0.5 cm). Data are shown as the mean ± SE. Results are representative of at least three independent experiments.

The wild-type (WT) strain and mutants, including those deleted in either or both *Mmd* and *Mir*, germinated at similar rates in a nutrient-rich medium, half-strength SDY (1/2SDY; Sabouraud dextrose broth plus yeast) (Fig. 2*A*). However, supplementing 1/2SDY with MeHg (0.2 mg/L) prevented germination of Δ*Mmd* and Δ*Mmd*::Δ*Mir*, while Mmd^{OE} and Mmd^{OE}::Mir^{OE} germinated significantly faster than the WT (Fig. 2*B*) ($P < 0.05$, by Tukey's test in one-way ANOVA). Only Mmd^{OE} and Mmd^{OE}::Mir^{OE} germinated with 0.3 mg MeHg/L (*SI Appendix*, Fig. S5), indicating that this level is above the tolerance of the WT.

Similarly, the WT and the diverse mutant strains showed no differences in mycelial growth rates on PDA (potato dextrose agar), but growth of Δ*Mmd* and Δ*Mmd*::Δ*Mir* was reduced by MeHg at 1 mg/L and completely blocked at 4 mg/L (Fig. 2). The MeHg concentration in soils that are regarded as badly contaminated is ∼1 mg/kg soil (13, 14). Only Mmd^{OE} and Mmd^{OE}::Mir^{OE} showed any growth at 16 mg MeHg/L (Fig. 2).

We similarly assayed tolerance to Hg^{2+}. At 10 or 15 mg Hg^{2+}/L, Mir^{OE} and Mmd^{OE}::Mir^{OE} had the fastest germination rates, while the WT and Mmd^{OE} germinated faster than Δ*Mir*, Δ*Mmd*, and Δ*Mmd*::Δ*Mir* (Fig. 2 and *SI Appendix*, Fig. S5) ($P < 0.05$, by Tukey's test in one-way ANOVA). At 20 mg/L, Δ*Mir*, Δ*Mmd*, and Δ*Mmd*::Δ*Mir* failed to germinate. Mir^{OE} and Mmd^{OE}::Mir^{OE} germinated significantly faster than Mmd^{OE}, which in turn germinated significantly faster than the WT (*SI Appendix*, Fig. S5) ($P < 0.05$, by one-way ANOVA). Therefore, *Mmd* and *Mir* both contribute to Hg^{2+} tolerance, even though the recombinant MMD protein does not reduce Hg^{2+} (*SI Appendix*, Fig. S1). We used qRT-PCR analysis to test the hypothesis that *Mmd* contributes to Hg^{2+} tolerance by changing the expression of *Mir*. Compared with the WT, the addition of Hg^{2+} increased *Mir* expression 5.6-fold in Mmd^{OE} and 14.7-fold in Mir^{OE}. In the absence of Hg^{2+}, *Mir* expression was similar in the WT and Mmd^{OE} but 3-fold less in Δ*Mmd*, suggesting that *Mir* expression is dependent on *Mmd*. The converse was not true; deletion of *Mir* had no impact on *Mmd* expression (*SI Appendix*, Fig. S3).

Mercury levels reach ∼30 mg Hg^{2+}/kg in polluted soils (14). Neither Δ*Mir* nor Δ*Mmd*::Δ*Mir* grew on PDA supplemented with 30 mg Hg^{2+}/L, whereas the other mutants showed WT levels of growth (Fig. 2). We also looked for any involvement of MMD and MIR in tolerance to other heavy metals and found no growth differences between the WT and mutant strains on PDA supplemented with Cd^{2+}, Cr^{2+}, Pb^{2+}, Cu^{2+}, Ag^{+}, or Fe^{3+} (*SI Appendix*, Fig. S6). Stress conferred by Cu^{2+}, Ag^{+}, or Fe^{3+} obviously inhibited colony growth and impaired conidiation, resulting in aberrant fluffy white colonies (*SI Appendix*, Fig. S6).

MMD and MIR Promote Symbiotic Interactions between Plants and *M. robertsii* under Mercury Stress. Several *Metarhizium* species, including *M. robertsii*, develop symbiotic associations with plant roots that increase plant growth, particularly under stress (15). We reasoned that tolerance to metals could also benefit *Metarhizium*'s partners in symbiotic associations. We thus assessed the mutants and WT for their ability to protect the major food crop maize (*Zea mays*) from mercury stress using as benchmarks plant growth and fungal colony-forming units (CFUs) in the rhizosphere and on roots. In normal soil, with no mercury supplementation, the WT and mutant strains

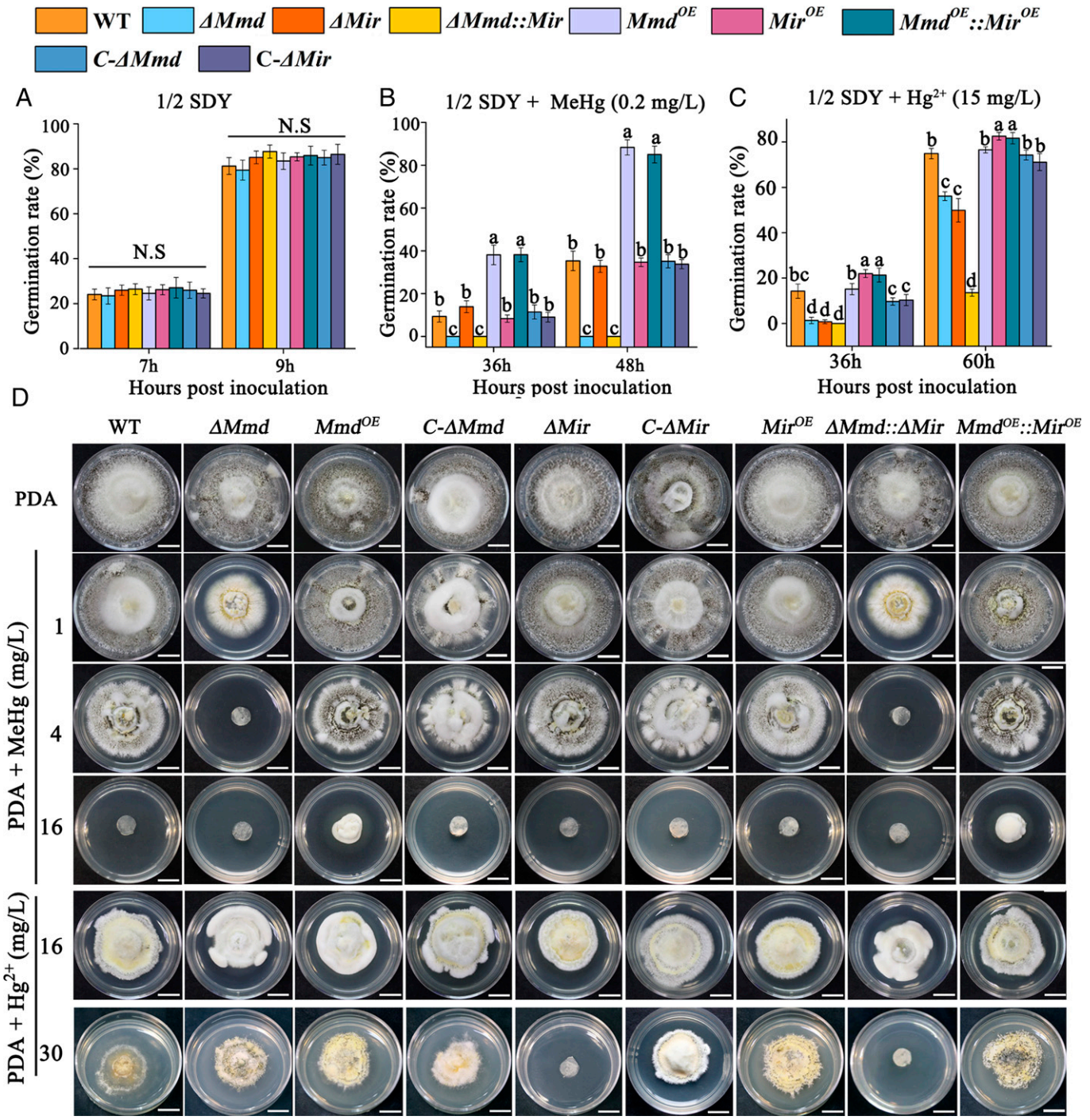

Fig. 2. MMD and MIR are involved in the mercury tolerance of *M. robertsii*. (*A*–*C*) Spore germination was measured in unamended 1/2SDY medium (*A*), 1/2SDY plus MeHg (0.2 mg/L) (*B*), and 1/2SDY plus Hg^{2+} (15 mg/L) (*C*). Data are expressed as the mean germination ± SE. Significant differences at a time point are indicated by different letters ($n = 3$; $P < 0.05$, by Tukey's test in one-way ANOVA). N.S, not significant. (*D*) Images were taken to show visual differences in colony growth of WT and mutant strains on PDA with or without either MeHg or Hg^{2+}. The mercury concentration (*Left*) and the strains (*Top*) are indicated. Pictures were taken 14 d after positioning a 5-mm-diameter mycelial plug on the center of each PDA plate. (Scale bars, 1 cm.) WT, the wild-type strain; Mmd^{OE}, overexpressing *Mmd*; Mir^{OE}, overexpressing *Mir*; $Mmd^{OE}::Mir^{OE}$, simultaneously overexpressing *Mmd* and *Mir*; Δ*Mmd*, *Mmd* deleted; Δ*Mir*, *Mir* deleted; Δ*Mmd*::Δ*Mir*, both *Mmd* and *Mir* deleted; *C*-Δ*Mmd* and *C*-Δ*Mir*, the complemented strains of Δ*Mmd* and Δ*Mir*, respectively.

(Δ*Mmd*, Δ*Mir*, Δ*Mmd*::Δ*Mir*, Mmd^{OE}, Mir^{OE}, and $Mmd^{OE}::Mir^{OE}$) had similar CFU counts and plant growth–promoting effects, suggesting that *Mmd* and *Mir* do not contribute to symbiotic interactions in uncontaminated soils (*SI Appendix*, Fig. S7). However, when grown with 15 μg MeHg/kg soil, a concentration found in heavily polluted soils (13), root CFU counts of Mmd^{OE} and $Mmd^{OE}::Mir^{OE}$ outnumbered those of the WT ∼1.4-fold, and the WT outnumbered Δ*Mmd* and Δ*Mmd*::Δ*Mir* ∼3.3-fold (Fig. 3). CFU counts of Mmd^{OE} and $Mmd^{OE}::Mir^{OE}$ also significantly outnumbered the WT in rhizospheric soils ($P < 0.05$, by Mann–Whitney *U* test), with Δ*Mmd* and Δ*Mmd*::Δ*Mir* being comparatively scarce (Fig. 3). Similarly, CFU counts of Δ*Mmd* and Δ*Mmd*::Δ*Mir* in bulk soil were significantly lower than the WT ($P < 0.05$, by Mann–Whitney *U* test) (*SI Appendix*, Fig. S8).

Mmd^{OE} or $Mmd^{OE}::Mir^{OE}$ gave the host maize significantly greater protection from mercury than the WT, reflected in the height of the plants as well as the dry weight of their roots and

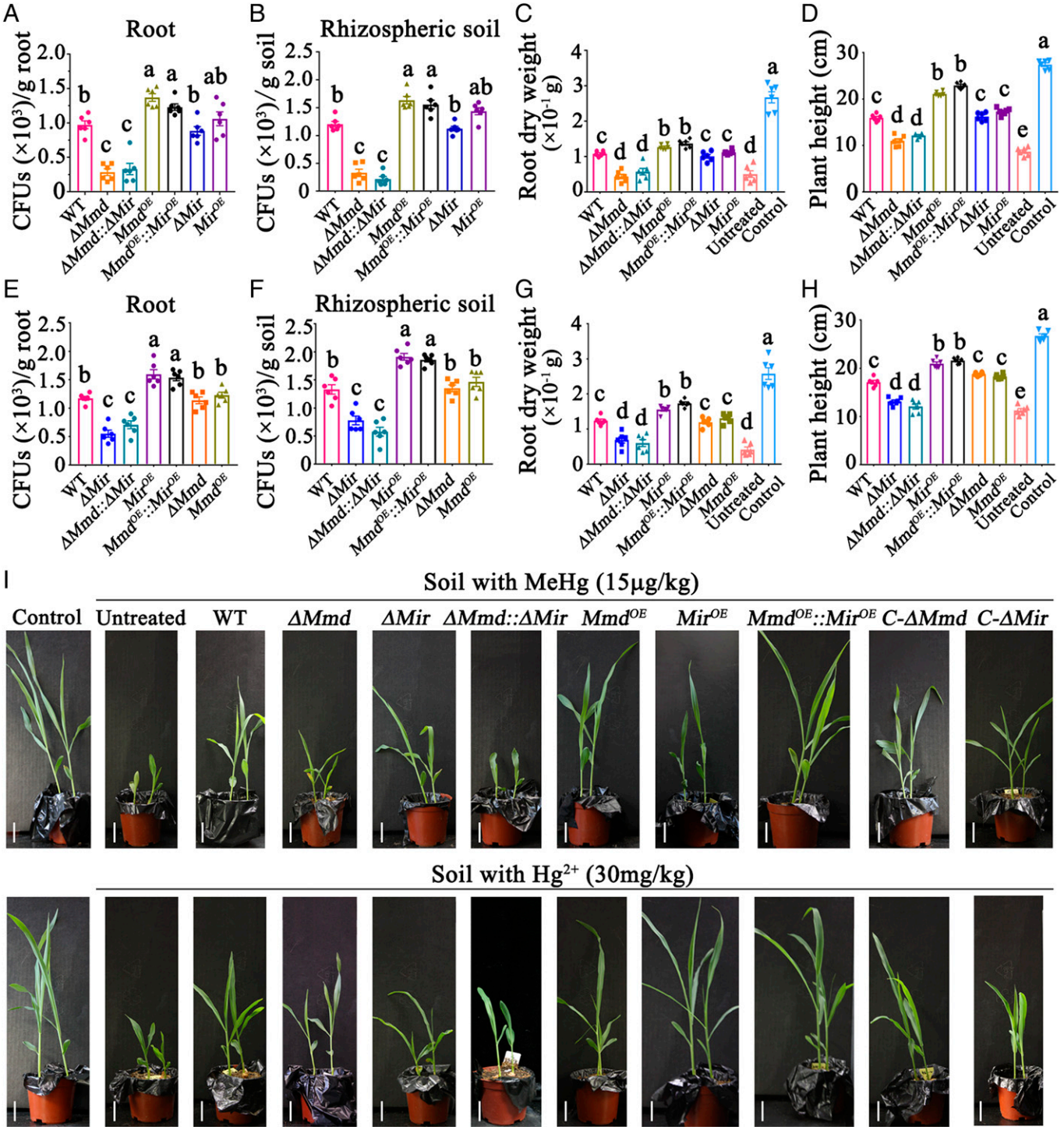

Fig. 3. MMD and MIR promote a mutually beneficial interaction between maize and *M. robertsii* under mercury stress. (*A–D*) Assessment of the impact of MeHg (15 μg/kg) in soil. Scatterplots show significant differences in CFU counts in the roots (*A*) and rhizospheric soil (*B*), and in root dry weight (*C*) and plant height (*D*) between the WT, gene deletion mutants, and overexpressors. (*E–H*) Assessment of the impact of Hg^{2+} (30 mg/kg) in soil. Significant differences between WT and transgenic strains were observed in CFU counts in the roots (*E*) and rhizospheric soil (*F*) that significantly impact root dry weight (*G*) and plant height (*H*). Data are expressed as the mean ± SE. Values with different letters are significantly different ($P < 0.05$, by Mann–Whitney *U* test). (*I*) Representative images showing visual differences between plants treated with WT and mutant strains in soil with MeHg (*Upper*) and Hg^{2+} (*Lower*). (Scale bars, 1 cm.) Data were collected at 10 dpi of fungal spore inoculation into the soil with maize plants. Untreated: plants not treated with a fungus; control: plants grown in normal soil without fungal treatment. Supplements to this figure are shown as *SI Appendix*, Figs. S8 and S10.

aboveground parts. The WT provided greater protection than Δ*Mmd* and Δ*Mmd::*Δ*Mir* (Fig. 3 and *SI Appendix*, Figs. S8 and S9). Compared with plants grown in unsupplemented soil, adding MeHg (10 μg/kg) reduced the dry weight of both the roots and aboveground parts >2.5-fold, but plants colonized with Mmd^{OE} or Mmd^{OE}::Mir^{OE} weighed the same as those in normal soil (*SI Appendix*, Fig. S9).

We also found that MIR promoted symbiotic interactions between *M. robertsii* and maize with 20 or 30 mg Hg^{2+}/kg of soil, typical of heavy pollution (14). CFU counts of the WT on the roots and in rhizospheric and bulk soils were significantly higher than those of the deletion strains Δ*Mir* and Δ*Mmd::*Δ*Mir* but significantly lower than those of the overexpressors Mir^{OE} and Mmd^{OE}::Mir^{OE} (Fig. 3 and

SI Appendix, Figs. S10 and S11) ($P < 0.05$, by Mann–Whitney *U* test).

Strong positive correlations ($r > 0.7$, $P < 0.0001$) were found between CFU counts and improved plant growth parameters under MeHg or Hg^{2+} stress (Fig. 4 and *SI Appendix*, Fig. S12). Thus, compared with WT-treated maize, the height and dry weights of the roots and aboveground parts were significantly increased with Mir^{OE} and Mmd^{OE}::Mir^{OE} but reduced with Δ*Mir* and Δ*Mmd*::Δ*Mir* (Fig. 3 and *SI Appendix*, Figs. S10 and S11) ($P < 0.05$, by Tukey's test in one-way ANOVA). Soil containing 20 mg Hg^{2+}/kg also greatly inhibited plant growth, but plants colonized by the overexpressors (Mir^{OE}, Mmd^{OE}, or Mmd^{OE}::Mir^{OE}) had the same dry weight of roots as those in soil without Hg^{2+} (*SI Appendix*, Fig. S11).

We then investigated whether *M. robertsii* nourished by maize roots cleans up MeHg and Hg^{2+} in soil and impacts mercury accumulation in plants. After 10 d, the MeHg concentration in rhizospheric soil from control plants not treated with a fungus was reduced from an initial 10 μg/kg to 8.1 μg/kg. This level was significantly reduced by the WT (6.6 μg/kg), and reduced significantly further (~5.1 μg/kg) by both Mmd^{OE} and Mmd^{OE}::Mir^{OE} (*SI Appendix*, Table S2) ($P < 0.05$, by Tukey's test in one-way ANOVA). Δ*Mir* and Mir^{OE} were similar in effect to the WT whereas Δ*Mmd* and Δ*Mmd*::Δ*Mir* did not reduce MeHg compared with controls (*SI Appendix*, Table S2). Negative correlations were found between CFU counts and MeHg concentration in rhizosphere soil (*SI Appendix*, Fig. S13). None of the fungal treatments significantly reduced the MeHg concentration in bulk soils, suggesting that bioremediation was localized to the vicinity of plant–fungus interactions (*SI Appendix*, Table S2).

We further found that *Mmd* reduced MeHg accumulation in plant tissues. The WT reduced MeHg 2.5-fold in roots compared with control plants untreated with fungi, with further (~3.8-fold) reductions achieved by the overexpressors Mmd^{OE} and Mmd^{OE}::Mir^{OE} ($P < 0.05$, by Tukey's test in one-way ANOVA). While Mir^{OE} reduced MeHg more than the WT ($P < 0.05$, by Tukey's test in one-way ANOVA), it was not as

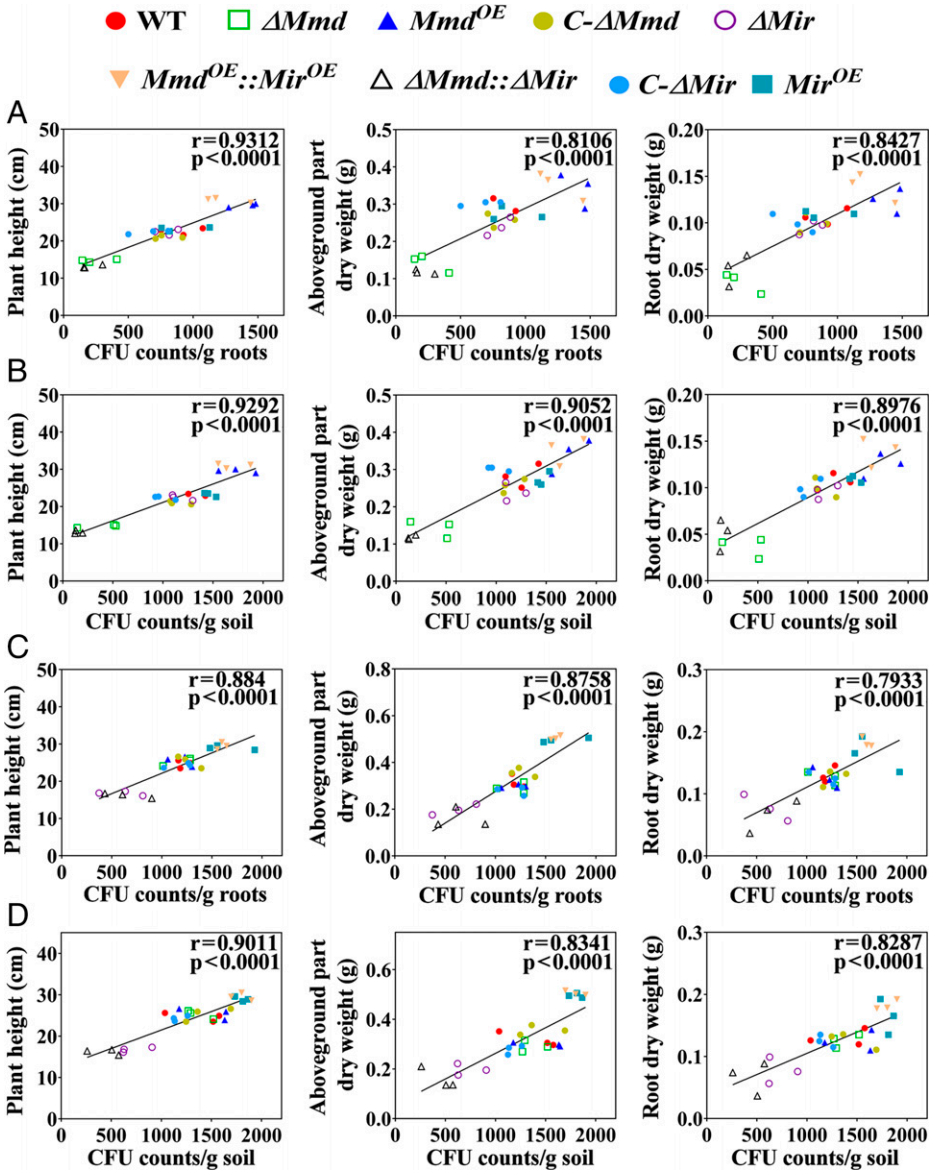

Fig. 4. Positive correlations between the CFU counts achieved by the WT and mutant strains and plant height and dry weight of roots and aboveground parts. Correlations between plant growth parameters and CFU counts per gram of roots (*A*) and rhizospheric soil (*B*) in soils with 15 μg MeHg/kg. The legends for *C* and *D* are the same as for *A* and *B*, respectively, except that the plants were grown in soil amended with 30 mg Hg^{2+}/kg. Correlation analysis was conducted with the Pearson's *r* correlation provided by GraphPad Prism v7.0 software.

effective as Mmd^{OE} (*SI Appendix*, Table S2), and the deletion strains Δ*Mmd* and Δ*Mmd*::Δ*Mir* were least effective at reducing MeHg accumulation (*SI Appendix*, Table S2) ($P < 0.05$, by Tukey's test in one-way ANOVA). Reductions in MeHg accumulation in roots were reflected in the aboveground foliage (*SI Appendix*, Table S2), with negative correlations between the CFU counts and accumulation of MeHg in plants (*SI Appendix*, Fig. S14). The accumulation of MeHg also negatively correlated with plant growth parameters (*SI Appendix*, Fig. S15).

Similar assays showed that root colonization by *M. robertsii* strains expressing MIR reduced soil Hg^{2+} and accumulation in plants. After 10 d, the rhizospheric Hg^{2+} level in the absence of a fungus was reduced from an initial 20 mg Hg^{2+}/kg to 17.2 mg/kg. This level was significantly reduced by the WT (14.7 mg/kg), and reduced significantly further (~12 mg/kg) by both Mir^{OE} and Mmd^{OE}::Mir^{OE} ($P < 0.05$, by Tukey's test in one-way ANOVA), whereas Δ*Mir* and Δ*Mmd*::Δ*Mir* had no significant impact. Thus, the WT, Mir^{OE}, and Mmd^{OE}::Mir^{OE} reduced Hg^{2+} accumulation in roots 6.2- to 9.2- and 10.9-fold, respectively, while compared with the WT, significantly more Hg^{2+} accumulated in roots treated with Δ*Mir* or Δ*Mmd*::Δ*Mir*. The *Mir*-mediated decrease in Hg^{2+} accumulation in roots was also found in the aboveground foliage (*SI Appendix*, Figs. S12–S15 and Table S2).

MMD and MIR Are Required for Bioremediation of Aqueous Solutions of MeHg and Hg^{2+}. We then explored the potential of *M. robertsii* mycelium (the WT and overexpressors Mmd^{OE}, Mir^{OE}, and Mmd^{OE}::Mir^{OE}) to remove MeHg and Hg^{2+} contamination from fresh and sea water. All four strains (1 g mycelium [dry weight]/L water) removed 1.5 mg MeHg from 1 L of fresh water in 48 h, and Mmd^{OE} and Mmd^{OE}::Mir^{OE} removed all MeHg at 2 mg/L, a pollutant level 1,000-fold higher than the limit (2 μg/L) recommended by the US Environmental Protection Agency (EPA) (16). After 48 h with an initial 5 mg MeHg/L, the WT, Mir^{OE}, Mmd^{OE}, and Mmd^{OE}::Mir^{OE} had reduced MeHg by 59, 58, 67, and 65%, respectively (*SI Appendix*, Fig. S16 and Table S3) ($P < 0.05$, by one-way ANOVA). One gram of the WT or Mir^{OE} mycelium removed ~2.9 mg of MeHg in 48 h, which was significantly lower than the ~3.3 mg removed by Mmd^{OE} and Mmd^{OE}::Mir^{OE} ($P < 0.05$, by Tukey's test in one-way ANOVA) (*SI Appendix*, Table S4).

All four strains (1 g mycelium [dry weight]/L water) also completely removed Hg^{2+} (0.5 mg/L) from fresh water within 48 h. Unlike the WT, Mmd^{OE}, Mir^{OE}, and Mmd^{OE}::Mir^{OE} were still able to completely clean up Hg^{2+} at 1 mg/L, which is 500-fold higher than the environmental limit (2 μg/L) set by the EPA (16). With 10 mg Hg^{2+}/L, the WT reduced Hg^{2+} 2-fold compared with control water untreated with fungi, with further (~2.9-fold) reductions achieved by the overexpressors Mir^{OE} and Mmd^{OE}::Mir^{OE} ($P < 0.05$, by Tukey's test in one-way ANOVA) (*SI Appendix*, Fig. S16 and Table S3). One gram of the Mmd^{OE}::Mir^{OE} or Mir^{OE} mycelium removed ~7.1 mg of Hg^{2+} in 48 h, which was significantly more than the ~6 mg removed by the WT and Mmd^{OE} ($P < 0.05$, by Tukey's test in one-way ANOVA) (*SI Appendix*, Table S4). Being in fresh or sea water did not affect removal of MeHg or Hg^{2+} by the WT but, at a high concentration (10 mg/L), the overexpressors Mir^{OE} and Mmd^{OE}::Mir^{OE} removed 6.5% more Hg^{2+} from fresh water. In nutrient medium (i.e., fresh water containing nutrients), overexpression of *Mmd* and *Mir* also increased the ability of *M. robertsii* to clean up MeHg and Hg^{2+} (*SI Appendix*, Fig. S16 and Tables S5–S7).

Fungi Containing MMD's Homologs Can Demethylate MeHg. A previous phylogenetic analysis showed that *Metarhizium* fungi may have acquired MMD from bacteria (11). In this study, an updated BLASTP analysis using MMD as a query identified homologs in six other *Metarhizium* species (*M. guizhouense*, *M. brunneum*, *M. humberi*, *M. anisopliae*, *M. acridum*, and *M. majus*) but not in earlier-diverged *Metarhizium* species such as *M. rileyi* and *M. album*. Homologs were also found in 15 phylogenetically distant non-*Metarhizium* species (*SI Appendix*, Table S8), 9 of which are known plant associates and the other 6 of which are soil fungi. Among the 15, the *Fusarium oxysporum* homolog (NW_022158525) showed the most similarity (55%) to MMD and *Amorphotheca resinae* (XP_024717523) showed the least (29%). Phylogenetic analysis suggested that the 15 MMD homologs derive from two different horizontal gene transfer events (*SI Appendix*, Fig. S17).

We then investigated whether *F. oxysporum*, *Cadophora malorum*, *A. resinae*, and five of the *Metarhizium* species with MMD homologs could also demethylate MeHg. *M. album*, *Beauveria bassiana*, and *Saccharomyces cerevisiae* lack MMD homologs and were used as controls. In a nutrient-rich medium with MeHg (50 μg/L), all MMD-containing species significantly reduced MeHg in the supernatant and mycelium compared with controls, and *M. robertsii*, *M. guizhouense*, and *M. brunneum* totally removed MeHg (*SI Appendix*, Table S9). Hg^{2+}, the product of MeHg demethylation, was also detected in the medium (*SI Appendix*, Table S9). *M. album*, *B. bassiana*, and *S. cerevisiae* had no impact on MeHg, and Hg^{2+} was not detected in the medium (*SI Appendix*, Table S9). Consistent with the presence of active MIR, all 12 MMD-containing or noncontaining species significantly reduced Hg^{2+} levels in the medium (*SI Appendix*, Table S10).

Finally, we showed that transformation of the *M. robertsii* *Mmd* gene into *B. bassiana* and *S. cerevisiae* allowed these two species to demethylate MeHg into Hg^{2+} (*SI Appendix*, Tables S11 and S12), and thus promoted their colony growth on solid media containing MeHg (*SI Appendix*, Figs. S18 and S19).

Discussion

In this study, we describe the genetic and biochemical mechanisms underlying mercury tolerance in the commercially important plant symbiotic fungus *M. robertsii*. MeHg is demethylated by the demethylase MMD into Hg^{2+}, which is subsequently reduced to elemental Hg through the Hg^{2+} reductase MIR. MIR homologs were found in many fungi, suggesting Hg^{2+} resistance conferred by MIR is widespread. However, MMD homologs were rare and patchily distributed among plant associates and soil fungi, and phylogenetic tracks suggest that they could have been acquired through two different evolutionary trajectories. MMD-mediated fungal resistance to MeHg could therefore be the result of convergent evolution by some soil fungi to survive mercury stress in their environment.

M. robertsii can develop mutually beneficial relationships with many diverse agriculturally important plants including maize, the world's most dominant and productive crop, where it is known to promote growth, suppress insect growth, and alter plant defense gene expression (17). In return, the plant roots provide a long-term habitat and a source of carbohydrates for the fungus (15). We found no evidence that either *Mmd* or *Mir* contributes to symbiotic interactions between *M. robertsii* and maize in normal soils. However, in MeHg- and Hg^{2+}-polluted soil, a fast-increasing threat to agriculture and ecosystems, detoxification of these Hg forms by MMD and MIR protects the fungus and

reduces mercury in plants, facilitating their growth. Therefore, MMD and MIR promote a mutually beneficial relationship between plants and *M. robertsii* under mercury stress, as reflected in the strong correlations between CFUs of the different *Metarhizium* mutant strains and plant growth. Given that emission of Hg from soil greatly affects the global Hg cycle (18) and plant symbiotic *Metarhizium* species are among the most abundant soil fungi (15), *Metarhizium* species with their host plants could represent an important branch of the global Hg cycle.

This also has important implications for potential bioremediation of Hg-polluted soil. *M. robertsii* can be applied to seeds before planting (19). This contrasts favorably with the bacterial sources of MMD and MIR, as these cannot reproduce in soil, and have yet to be used for bioremediation (20). There is an extra dimension in the quality of the interactions between fungi and plants as, unlike bacteria, fungi can grow and spread through the rhizosphere as hyphal growth. However, bioremediation appears limited to the vicinity of roots, where the fungus is localized, which will also localize and limit the release of volatile elemental mercury. If required, release of volatile mercury could be further contained by applying sorbents such as activated carbon on the surface of the soil overlying the root system. Ease of cultivation and genetic manipulation of *M. robertsii* means the ability to remove MeHg and Hg^{2+} can also be enhanced by the simple expedient of overexpressing MMD and MIR. In countries that are unfavorably disposed to transgenic products, it may be possible to use chemical mutagenesis and/or artificial selection to enhance production of MMD and MIR. Multiple *Metarhizium* species can efficiently demethylate MeHg and reduce Hg^{2+}, and can develop symbiotic relationships with diverse plants including grasses, trees, vegetables, and crops (17, 21). However, there is evidence for coevolution with plants in that *M. robertsii* preferentially associates with the roots of grasses, *M. brunneum* with shrubs, and *M. guizhouense* with trees (22). So, plants and *Metarhizium* species could be combined in optimal pairs for cleaning up MeHg and Hg^{2+} in different types of polluted soil.

Furthermore, *Metarhizium* mycelium efficiently removes MeHg and Hg^{2+} in water at concentrations >1,000-fold (MeHg) and 500-fold (Hg^{2+}) higher than the limit (2 μg/L) recommended by the EPA (16). Unlike bacteria that usually require nutrients to remediate Hg-contaminated water (20), *M. robertsii* did not require any additional supplements. *Metarhizium* fungi have a long history of being used as biocontrol agents against insect pests, and their safety to humans and the environment has been clearly established through several decades of high-quality research (23). In addition, industrial production of *Metarhizium* for insect pest control is highly automated and cost-effective (24). Therefore, *Metarhizium* fungi seem well-placed to help manage a complex and unprecedented set of dangerous environmental trends.

Materials and Methods

Microorganisms and Plants. *M. robertsii* (ARSEF2575), *M. guizhouense* (ARSEF977), *M. brunneum* (ARSEF3297), *M. anisopliae* (ARSEF549), *M. acridum* (ARSEF324), *M. majus* (ARSEF977), and *M. album* (ARSEF1940) were from the Agricultural Research Service Collection of Entomopathogenic Fungi (ARSEF) in Ithaca, NY. *F. oxysporum* was from the Agricultural Research Service Culture Collection (NRRL 32931) in Peoria, IL. *C. malorum* was from the Centraalbureau voor Schimmelcultures (CBS 100591) in The Netherlands. *A. resinae* was also from the Centraalbureau voor Schimmelcultures (CBS 186.54). Details of the fungal strains are listed in *SI Appendix*, Table S1.

E. coli strain DH5α and *Agrobacterium tumefaciens* AGL1 were used for plasmid construction and fungal transformation, respectively (25). *E. coli* strain BL21 was used for expression of the recombinant MMD and MIR proteins.

Maize (*Z. mays*) seeds (Zhongnongtian 488) were commercially purchased (Beijing Huanai Agricultural Development).

Expression and Purification of MMD and MIR. The coding sequences of MMD and MIR were cloned with PCR using High-Fidelity Taq DNA polymerase (KOD Plus Neo). All PCR products were confirmed by sequencing. The MMD clone was inserted into the *Eco*RI/*Bam*HI site of the plasmid pET-SUMO (Invitrogen). The resulting plasmid pET-SUMO-MMD was then transferred into the *E. coli* BL21 (DE3) strain, and expression of MMD was induced by IPTG (isopropyl β-D-1-thiogalactopyranoside) at 18 °C for 12 to 16 h as described in the manufacturer's instructions (Novagen). The crude extract was prepared as previously described (11), and subjected to sodium dodecyl sulfate–polyacrylamide-gel electrophoresis and Western blot analysis with the anti–His tag antibody (HUABIO) to verify the expression of MMD. The recombinant SUMO:MMD was first purified with HisPur Ni-NTA resin (Thermo Scientific), and the His and SUMO tags were then removed with laboratory-prepared SUMO protease ULP1. The native protein was then purified to homogeneity with HisPur Ni-NTA resin and centrifugation with Amino Ultra-15 (10 kDa) (Millipore). Glycerol was added to the purified protein fraction at a final concentration of 10%.

The PCR-cloned coding sequence of MIR was inserted into the *Eco*RI site of the plasmid pET-SUMO to produce the plasmid pET-SUMO-MIR. The expression of the recombinant SUMO::MIR protein and purification with HisPur Ni-NTA resin were conducted as described above. Since hydrolysis of the protease ULP1 caused a dramatic loss of the SUMO::MIR protein, this fusion protein was directly used for biochemical characterization after a second purification by centrifugation with Amino Ultra-15 (10 kDa) (Millipore). All primers used in this study are listed in *SI Appendix*, Table S13.

Biochemical Characterization of MMD and MIR. The ability of MMD to demethylate MeHg was measured as described (26). Briefly, a 200-μL reaction mixture of 50 mM sodium phosphate buffer (pH 7.4) containing MeHg (0.5, 1, 2, 4, or 8 μM), the MMD protein (5 μg), ethylenediaminetetraacetate (EDTA) (5 mM, pH 7.0), magnesium acetate (0.2 mM), L-cysteine (0.5 mM), and bovine serum albumin (BSA) (0.5 mg/mL) was incubated at 37 °C for 1 h. High performance liquid chromatography-inductively coupled plasma-mass spectrometry (HPLC-ICP-MS) was used to quantify MeHg and Hg^{2+}, the product of demethylation of MeHg. The technical details of HPLC-ICP-MS are described below. A unit of activity was determined as the amount of Hg^{2+} produced in 1 min. We used GraphPad Prism v7.0 to create a Lineweaver–Burk plot and calculate V_{max} and K_m values using double-reciprocal transformation. The production of Hg^{2+} was also visualized using the $SnCl_2$ precipitation method as described (27). The $SnCl_2$ solution (10%) was prepared in 30% HCl; 2 μL was added into the MeHg demethylation reaction mixture (1 mL), which was then incubated at 37 °C for 10 min; 1 mL of the sodium phosphate buffer (pH 7.4) containing Hg^{2+} (10 mg) was used as a positive control. The white precipitate was then collected by centrifugation for observation.

The ability of MIR to reduce Hg^{2+} was measured as described (26). Two hundred microliters of 50 mM sodium phosphate buffer (pH 7.4) containing Hg^{2+} (0, 2, 4, 8, or 16 μM), the SUMO::MIR protein (10 μg), EDTA (5 mM, pH 7.0), magnesium acetate (0.2 mM), L-cysteine (0.5 mM), BSA (0.5 mg/mL), and NADPH (200 μM) was incubated at 37 °C for 2 h. HPLC-ICP-MS was used to quantify Hg^{2+}. A unit of activity was determined as the amount of Hg^{2+} consumed in 1 min. The Lineweaver–Burk plot V_{max} and K_m values were calculated as described for MMD.

Gene Deletion. Deletions of the *Mmd* or *Mir* gene based on homologous recombination were conducted as previously described (25). Ppk2-bar-GFP (11) was used to construct the gene deletion plasmid used to delete *Mir* in the WT strain to produce Δ*Mir*. To complement Δ*Mir*, a DNA fragment containing the promoter, open reading frame, and downstream terminator region of *Mir* was cloned by PCR using *M. robertsii* genomic DNA as the template, and recombined into the plasmid pPK2-Sur-GFP (11). The resulting plasmid was then transferred into the deletion mutant to construct the complemented strain C-Δ*Mir*. The double–gene deletion mutant Δ*Mmd*::Δ*Mir* was constructed by deleting *Mir* in the deletion mutant Δ*Mmd* using the deletion plasmid constructed with the master plasmid Ppk2-NTC-GFP (11).

qRT-PCR Analysis. Total RNA in the mycelium was extracted with TRIzol reagent (Life Technologies). For qRT-PCR analysis, complementary DNA was synthesized using ReverTra Ace qPCR RT Master Mix (Toyobo). qPCR analysis was performed using Thunderbird SYBR qPCR Mix without ROX (Toyobo). The reference genes and methods for calculating the relative expression level of each gene were

previously described (28). All qRT-PCR experiments were repeated three times. The primers for qRT-PCR analysis are shown in *SI Appendix*, Table S13.

Construction of *Metarhizium* Strains Overexpressing *Mmd* or *Mir* and Strains of *S. cerevisiae* and *B. bassiana* Heterologously Expressing *Mmd*. The PCR-cloned coding sequence of MMD was inserted into the *Eco*RV site in the binary expression plasmid pPk2-sur-GFP-T (29) to produce pPk2-sur-GFP-Mmd, in which the *Mmd* gene is driven by the constitutive promoter *Ptef* from *Aureobasidium pullulans* (30). The *Mmd* expression plasmid was incorporated into *A. tumefaciens* cells for *M. robertsii* and *B. bassiana* transformation to produce the strains Mmd^{OE} and *Bb-Mmd*, respectively. A PCR-cloned MIR coding sequence was inserted into the binary expression plasmid pPk2-bar-GFP-T (29) to produce pPk2-bar-GFP-Mir, which was then transformed into both WT *M. robertsii* and Mmd^{OE}, resulting in the strains Mir^{OE} and Mir^{OE}::Mmd^{OE}, respectively. Overexpression of *Mmd* and *Mir* in *M. robertsii* was confirmed by qRT-PCR analysis as described below. Heterologous expression of *Mmd* was confirmed with RT-PCR.

To constitutively express *Mmd* in *S. cerevisiae*, the coding sequence of MMD was amplified with PCR and cloned into the yeast plasmid pAdh1 (31) to produce pAdh1-Mmd, which was then transformed into *S. cerevisiae* strain BY4741, resulting in the strain *Sc-Mmd*. Successful transformation of pAdh1-Mmd into yeast cells was confirmed with PCR.

Assaying Microbial Tolerance to MeHg and Hg^{2+}. Tolerance of *M. robertsii* to MeHg and Hg^{2+} was assayed by inoculating spores (1.5×10^6) into 30-mm-diameter Petri dishes containing 2 mL of 1/2SDY medium supplemented with either MeHg or Hg^{2+}.

Mycelial tolerance of *M. robertsii* and *B. bassiana* was also tested. To this end, 100 μL of a spore suspension (1×10^7 conidia per milliliter) was evenly spread onto a PDA plate (90 mm in diameter). After a 3-d incubation at 26 °C, an agar plug with mycelium (5 mm in diameter) was transferred to the center of a new PDA plate supplemented with MeHg or Hg^{2+}.

Tolerance of *S. cerevisiae* and *E. coli* to MeHg was assayed by measuring colony growth on MeHg-containing solid synthetic defined (SD) (without uracil) or Luria Bertani (LB) medium with kanamycin, respectively. Yeast cultures were grown in liquid SD (without uracil) to an optical density of 600 nm (OD_{600nm}) of ∼1.0, which was then diluted and spotted onto solid SD (without uracil) medium supplemented with MeHg. Overnight *E. coli* cultures were diluted to an OD_{600nm} of ∼0.1 in 10 mL of LB, and further cultured for 2 to ∼3 h to achieve an OD_{600nm} of ∼0.8 to ∼1.0. IPTG was then added to a final concentration of 0.8 mM. After 12 h to induce the expression of the fusion protein SUMO::MMD, the OD_{600nm} of the culture was adjusted to 1.0, the culture was centrifuged (6,000 rpm for 5 min), and the pellet from 1 mL of culture was resuspended in 1 mL of an NaCl solution (0.09%). The resulting cell suspension was then spotted onto solid LB medium supplemented with MeHg and kanamycin. Each stress tolerance assay was repeated three times with three replicates per repeat.

Quantification of MeHg and Hg^{2+}. MeHg and Hg^{2+} were quantified using HPLC-ICP-MS analysis as described (32), using an Agilent Infinity 1260 II with a Zorbax Eclipse Plus C-18 column (150 × 4.6 mm) at a flow rate of 1 mL/min. The mobile-phase solution was prepared by mixing solution A (NH_4Ac [10 mM], L-cysteine [0.12%], pH 7.5) and solution B (methanol) at a ratio of 98:2. ICP-MS analysis was conducted on an Agilent Technologies 7800 ICP-MS instrument with a radio frequency power of 1,550 w, 100 μL/min paraformaldehyde, sample depth of 4.5 mm, carrier gas flow rate of 0.75 L/min, makeup gas flow rate of 0.4 L/min, plasma gas flow rate of 17 L/min, nebulizer gas flow rate of 1 L/min, and gas channel of 5.0 mL/min He. A quartz spray chamber and Scott double-pass were used.

MeHg and Hg^{2+} in biological samples were prepared as described (33). The mycelium of filamentous fungi was dried by lyophilization, weighed, and digested overnight in an ampule of HCl solution (6 M), which was then treated in an ultrasonic bath (70 kHz; Elma) for 1 h at room temperature. The resulting mixture was diluted 10-fold with distilled water, filtered through a membrane (pore size 0.22 μm), and further diluted 10-fold with the HPLC mobile-phase solution before HPLC-ICP-MS analysis.

Yeast cells grown in 1 mL of SD medium to an OD_{600nm} of 1.0 were harvested by centrifugation (6,000 rpm for 5 min), and treated with HCl as described above for mycelium. Soil samples were similarly treated with HCl.

To prepare MeHg and Hg^{2+} from roots and aboveground parts of plants, plant tissues were lyophilized, weighed, ground into a fine powder under liquid nitrogen, and subjected to digestion in HCl as described for the mycelium.

To assay MeHg and Hg^{2+} in liquids, samples were diluted 100-fold with the HPLC mobile-phase solution, and then filtered through a membrane (pore size 0.22 μm) before HPLC-ICP-MS analysis.

Bioremediation of MeHg- and Hg^{2+}-Polluted Water with a Fungal Mycelium. The ability of fungal mycelia to bioremediate MeHg- and Hg^{2+}-polluted water with nutrients and without nutrients was assayed. Mycelium was prepared by inoculating 10^8 spores in 100 mL of SDY broth followed by a 36-h incubation at 26 °C with 220-rpm shaking. The mycelium was then harvested by filtration, weighed, and resuspended in water with MeHg or Hg^{2+}. After a 48-h treatment, MeHg and Hg^{2+} in the supernatant and mycelium were quantified. The types of water assayed were regular distilled water, sea water prepared by dissolving sea salt (2.24%; Red Sea Fish Pharm) in distilled water, and SDY medium that contains nutrients in distilled water. This experiment was repeated three times with three replicates per repeat.

Bioremediation of MeHg- and Hg^{2+}-Polluted Soil by *M. robertsii*–Colonizing Maize Roots. We then assayed the ability of *M. robertsii* nourished by maize to bioremediate MeHg- and Hg^{2+}-polluted soil and thereby reduce mercury bioaccumulation in plants. To do this, maize seeds were surface-sterilized by soaking first in a sodium hypochlorite (NaOCl) solution (0.4%, 5 min) and then in hydrogen peroxide (15%, 10 min), before washing with sterile distilled water. The sterilized seeds were maintained on 2% water agar at 4 °C for ∼16 h to synchronize germination, and then at 24 °C to allow germination. Two germinated seedlings per plastic garden pot (7 cm in height by 10 cm in diameter) were planted in sterile soil containing MeHg or Hg^{2+}. The sterile soil was a mixture of peat soil (Klasmann-Deilmann, 876), domestic nutrient soil, and vermiculite. After a 4-d cultivation in a greenhouse (25 °C, photoperiod of 16 h light:8 h dark), 10 mL of spore suspension (1×10^5 spores per milliliter) was inoculated into the vicinity of the roots, and the plants were returned to the greenhouse. At 10 d postinoculation (dpi), the rhizosphere soil, roots, and aboveground parts of the plant were harvested for quantification of MeHg and Hg^{2+} as described above. The plant height as well as the dry biomass of both the roots and aboveground parts were also measured. Colonization of the rhizosphere and roots was assayed as described (31). Briefly, to assay root colonization, the roots were washed free of soil with sterile water, dried with sterilized tissue paper, weighed, and homogenized in a Triton X-100 solution (0.05%). The resulting homogenate was then plated onto a *Metarhizium* selective medium (31), and CFUs were counted to quantify root colonization. Soil attached to the roots (rhizosphere soil) was also collected in Triton X-100 solution and plated on the selective medium; CFUs were counted to quantify rhizosphere competency. This experiment was repeated six times with two plants (replicates of each treatment) per repeat.

Phylogenetic Analysis. MMD and MIR were used as queries to identify their respective fungal and bacterial homologs for phylogenetic analysis. Protein sequences were aligned using MUSCLE v3.7 with default parameters (34). The alignments were then manually refined and end-trimmed to eliminate poor alignments and divergent regions. Unambiguously aligned positions were used for construction of a maximum-likelihood (ML) tree with MEGA v7.0 (gap treatment: use all sites; models of evolution: WAG+G+I+F for MMD and LG+I for MIR; 100 bootstrap replications) (35). A neighbor-joining tree with default parameters (gap treatment: pairwise deletion; 1,000 bootstrap replications) was also constructed with MEGA v7.0. We also constructed a Bayesian inference tree with MrBayes v3.2.5 as described (11, 36); the models of evolution for MMD and MIR were the same as those used for ML tree construction.

Statistical Analysis. Normality was checked with the Shapiro–Wilk test with SPSS 20.0. If the data followed normal distribution, the Tukey's test in one-way ANOVA was carried out to evaluate the differences among multiple treatments ($\alpha = 0.05$). If the data were not normally distributed, the Mann–Whitney test *U* was performed. The Tukey's test and the Mann–Whitney *U* test were performed with GraphPad Prism v7.0.

Data, Materials, and Software Availability. All study data are included in the article and/or *SI Appendix*.

ACKNOWLEDGMENTS. This work was supported by a National Natural Science Foundation of China Grant (32172470).

1. C. T. Driscoll, R. P. Mason, H. M. Chan, D. J. Jacob, N. Pirrone, Mercury as a global pollutant: Sources, pathways, and effects. *Environ. Sci. Technol.* **47**, 4967–4983 (2013).
2. P. F. Schuster *et al.*, Permafrost stores a globally significant amount of mercury. *Geophys. Res. Lett.* **45**, 1463–1471 (2018).
3. K. M. Rice, E. M. Walker Jr., M. Wu, C. Gillette, E. R. Blough, Environmental mercury and its toxic effects. *J. Prev. Med. Public Health* **47**, 74–83 (2014).
4. J. L. O'Donoghue *et al.*, Neuropathology associated with exposure to different concentrations and species of mercury: A review of autopsy cases and the literature. *Neurotoxicology* **78**, 88–98 (2020).
5. M. S. Bank, The mercury science-policy interface: History, evolution and progress of the Minamata Convention. *Sci. Total Environ.* **722**, 137832 (2020).
6. J. M. Parks *et al.*, The genetic basis for bacterial mercury methylation. *Science* **339**, 1332–1335 (2013).
7. A. L. Fox *et al.*, Mercury biomagnification in food webs of the northeastern Chukchi Sea, Alaskan Arctic. *Deep Sea Res. Part II Top. Stud. Oceanogr.* **144**, 63–72 (2017).
8. M. Priyadarshanee, S. Chatterjee, S. Rath, H. R. Dash, S. Das, Cellular and genetic mechanism of bacterial mercury resistance and their role in biogeochemistry and bioremediation. *J. Hazard. Mater.* **423**, 126985 (2022).
9. M. Słaba, P. Bernat, S. Różalska, J. Nykiel, J. Długoński, Comparative study of metal induced phospholipid modifications in the heavy metal tolerant filamentous fungus *Paecilomyces marquandii* and implications for the fungal membrane integrity. *Acta Biochim. Pol.* **60**, 695–700 (2013).
10. M. Miransari, Hyperaccumulators, arbuscular mycorrhizal fungi and stress of heavy metals. *Biotechnol. Adv.* **29**, 645–653 (2011).
11. Q. Zhang *et al.*, Horizontal gene transfer allowed the emergence of broad host range entomopathogens. *Proc. Natl. Acad. Sci. U.S.A.* **116**, 7982–7989 (2019).
12. I. N. Krout, T. Scrimale, D. Vorojeikina, E. S. Boyd, M. D. Rand, Organomercurial lyase (MerB)-mediated demethylation decreases bacterial methylmercury resistance in the absence of mercuric reductase (MerA). *Appl. Environ. Microbiol.* **88**, e0001022 (2022).
13. T. Tomiyasu *et al.*, The dynamics of mercury near Idrija mercury mine, Slovenia: Horizontal and vertical distributions of total, methyl, and ethyl mercury concentrations in soils. *Chemosphere* **184**, 244–252 (2017).
14. X. Feng, G. Qiu, Mercury pollution in Guizhou, southwestern China–An overview. *Sci. Total Environ.* **400**, 227–237 (2008).
15. R. J. St. Leger, J. B. Wang, *Metarhizium*: Jack of all trades, master of many. *Open Biol.* **10**, 200307 (2020).
16. EPA, https://www.epa.gov/ground-water-and-drinkingwater/table-regulated-drinking-water-contaminants#Inorganic (2016). Accessed 16 March 2022.
17. I. Ahmad, M. del Mar Jiménez-Gasco, D. S. Luthe, S. N. Shakeel, M. E. Barbercheck, Endophytic *Metarhizium robertsii* promotes maize growth, suppresses insect growth, and alters plant defense gene expression. *Biol. Control* **144**, 104167 (2020).
18. B. Gworek, W. Dmuchowski, A. H. Baczewska-Dąbrowska, Mercury in the terrestrial environment: A review. *Environ. Sci. Eur.* **32**, 128 (2020).
19. X. Liao, T. R. O'Brien, W. Fang, R. J. St. Leger, The plant beneficial effects of *Metarhizium* species correlate with their association with roots. *Appl. Microbiol. Biotechnol.* **98**, 7089–7096 (2014).
20. K. R. Mahbub *et al.*, Bioremediation of mercury: Not properly exploited in contaminated soils! *Appl. Microbiol. Biotechnol.* **101**, 963–976 (2017).
21. S. Moonjely, L. Barelli, M. J. Bidochka, Insect pathogenic fungi as endophytes. *Adv. Genet.* **94**, 107–135 (2016).
22. M. Wyrebek, C. Huber, R. K. Sasan, M. J. Bidochka, Three sympatrically occurring species of *Metarhizium* show plant rhizosphere specificity. *Microbiology (Reading)* **157**, 2904–2911 (2011).
23. H. Zhao, B. Lovett, W. Fang, Genetically engineering entomopathogenic fungi. *Adv. Genet.* **94**, 137–163 (2016).
24. R. J. St. Leger, From the lab to the last mile: Deploying transgenic approaches against mosquitoes. *Front. Trop. Dis.*, https://doi.org/10.3389/fitd.2021.804066 (2021).
25. C. Xu *et al.*, A high-throughput gene disruption methodology for the entomopathogenic fungus *Metarhizium robertsii*. *PLoS One* **9**, e107657 (2014).
26. J. L. Schottel, The mercuric and organomercurial detoxifying enzymes from a plasmid-bearing strain of *Escherichia coli*. *J. Biol. Chem.* **253**, 4341–4349 (1978).
27. F. Effenberger, G. Kiefer, Stereochemistry of the cycloaddition of sulfonyl isocyanates and *N*-sulfinylsulfonamides to enol ethers. *Angew. Chem. Int. Ed.* **6**, 951–952 (1967).
28. W. Fang, M. J. Bidochka, Expression of genes involved in germination, conidiogenesis and pathogenesis in *Metarhizium anisopliae* using quantitative real-time RT-PCR. *Mycol. Res.* **110**, 1165–1171 (2006).
29. X. Zhang, Y. Meng, Y. Huang, D. Zhang, W. Fang, A novel cascade allows *Metarhizium robertsii* to distinguish cuticle and hemocoel microenvironments during infection of insects. *PLoS Biol.* **19**, e3001360 (2021).
30. R. N. Spear, D. Cullen, J. H. Andrews, Fluorescent labels, confocal microscopy, and quantitative image analysis in study of fungal biology. *Methods Enzymol.* **307**, 607–623 (1999).
31. J. Dai *et al.*, The sugar transporter MST1 involved in colonization of rhizosphere and rhizoplane by *Metarhizium robertsii*. *mSystems* **6**, e0127721 (2021).
32. D. Chen, M. Jing, X. Wang, Determination of methylmercury in water and soil by HPLC-ICP-MS (2005). https://www.agilent.com/cs/library/applications/5989-3572EN.pdf. Deposited 6 March 2005.
33. K. Leopold, M. Foulkes, P. Worsfold, Methods for the determination and speciation of mercury in natural waters–A review. *Anal. Chim. Acta* **663**, 127–138 (2010).
34. R. C. Edgar, MUSCLE: Multiple sequence alignment with high accuracy and high throughput. *Nucleic Acids Res.* **32**, 1792–1797 (2004).
35. S. Kumar, G. Stecher, K. Tamura, MEGA7: Molecular evolutionary genetics analysis version 7.0 for bigger datasets. *Mol. Biol. Evol.* **33**, 1870–1874 (2016).
36. F. Ronquist *et al.*, MrBayes 3.2: Efficient Bayesian phylogenetic inference and model choice across a large model space. *Syst. Biol.* **61**, 539–542 (2012).